International Journal of Heat and Mass Transfer 86 (2015) 744–754

Contents lists available at ScienceDirect

International Journal of Heat and Mass Transfer

journal homepage: www.elsevier.com/locate/ijhmt

Nucleate pool boiling and filmwise condensation heat transfer of R134a on the same horizontal tubes

Wen-Tao Ji [a], Mitsuharu Numata [b], Ya-Ling He [a], Wen-Quan Tao [a,*]

[a] Key Laboratory of Thermo-Fluid Science and Engineering of MOE, Xi'an Jiaotong University, Xi'an 710049, China
[b] Environmental Technology Lab, Daikin Industries, Ltd., Japan

ARTICLE INFO

Article history:
Received 12 September 2014
Received in revised form 9 February 2015
Accepted 9 February 2015
Available online 2 April 2015

Keywords:
Pool boiling
Condensing
Heat transfer
R134a
Tube

ABSTRACT

Pool boiling and condensing heat transfer of R134a on one plain and three enhanced surfaces are experimentally investigated. The saturation temperature in pool boiling is 6 °C and condensing is 40 °C. The heat flux ranges from 8 to 86 kW/m^2. The enhanced tubes include integral-fin, pyramid and re-entrant cavity surface. The outside diameter of test tubes is 19 mm and the length of test section for boiling is 1100 mm and condensing is 1800 mm. Integral-fin tube has lower heat transfer coefficient in boiling and condensing. The deviations of experiment result and Owen or Webb models are within ±10% for integral-fin tube in condensing. Pyramid surface provides quite close heat transfer coefficient with re-entrant cavity surface in pool boiling and condensing at heat flux greater than 70 kW/m^2. The heat transfer performances of re-entrant cavity surface tube is the highest among the three enhanced tubes in either pool boiling or condensing at not high heat flux. The heat transfer coefficients can be 1.9–4.8 and 14.8–19.3 times those of a plain tube in pool boiling and condensing respectively. The decreasing rate of heat transfer coefficient for re-entrant cavity surface is also higher than pyramid surface in condensing. Literature survey on nucleate pool boiling and filmwise condensation is also conducted.

1. Introduction

Boiling and filmwise condensation are two basic heat transfer modes in power, chemical process and HVAC systems. It assumed an important role in heat transfer applications. Recent interest has centered on the requirements of more compact and efficient heat exchangers. For shell and tube condenser and flooded evaporator in the larger capacity HVAC system, water flows through the tube side and refrigerant is condensing or boiling in the shell side. To enhance the phase-change heat transfer, two independent methods have been established and different heat transfer surfaces were designed in the recent decades. According to [1–6], the basic principle for the enhancement of pool boiling is trying to increase the number of nucleation sites over a long period. While for filmwise condensation, it is to reduce the thickness of film using sharp edges and increase the effective heat transfer area outside the condensing surface.

Following review of the state of art mainly concerns the heat transfer performance of cross-grooved tubes. It is presented here in the sequence of nucleate pool boiling and film condensation.

Many enhanced geometries have been developed so far for improvement of pool boiling heat transfer. Thermoexcel-E [7], Tuobo-B [8,9], Gewa-T [10] and Everfin-Δ [11] are some commercial tubes for nucleate pool boiling heat transfer. For the enhanced tubes, it is found that heat transfer coefficients increase with heat flux. The enhancement ratios (h_e/h_p) decrease with increasing heat flux. Higher heat transfer augmentation is obtained with reentrant cavity tubes. Nucleate sites may occur somewhere inside the cavity and bubbles grow outside of cavity when the wall temperature exceeds the activation superheat. Mouth size and depth of cavity are important parameters to influence the pool boiling heat transfer [12].

Webb and Pais [8] studied the pool boiling of five refrigerants on five different horizontal tube geometries. The tube geometries include a plain, a standard 26 fpi (fins per inch) low-fin, and three commercially available three dimensional enhanced tubes (Gewa-TX19, Gewa-SE, and Turbo-B). Tests were performed at two saturation temperatures of 4.44°C and 26.7°C with refrigerants R11, R12, R22, R123 and R134a. For refrigerant R134a and heat flux in the range of 8.4–62.2 kW/m^2, Turbo-B had the highest heat transfer coefficient over the other 3 enhanced tubes. The heat transfer coefficient was 4.7–2.9 times over plain tube in the range of 10.4–22.1 kW/m^{2}K. As the increment of heat flux, the

* Corresponding author.
E-mail address: wqtao@mail.xjtu.edu.cn (W.-Q. Tao).

http://dx.doi.org/10.1016/j.ijheatmasstransfer.2015.02.020
0017-9310/

List of symbols

a	coefficient of equation
A	area, m^2
b	coefficient of equation
c_i	enhanced ratio of inside heat transfer coefficient
c_p	specific heat capacity, J/kg K
C	coefficient of Cooper equation
d	diameter of tube, mm
e	height of outside fin, mm
f	drag coefficient
g	gravitational acceleration, m/s^2
h	heat transfer coefficients, W/m^2K
H	height of inside fin, mm
k	overall heat transfer coefficients, W/m^2 K
L	tube's tested length, m
m	mass flow rate, kg/s
M_r	molecular weight of refrigerant
Pr	prandtl number in Gnielinski equation; Reduced pressure in Cooper equation
q	heat flux, W/m^2
Re	*Reynolds* number
R_f	thermal resistance of foul
R_P	average surface roughness of plain tube, m
R_w	thermal resistance of tube wall, m^2K/W
T	temperature, °C

Greek alphabet

ϕ	heat transfer rate, W
α	helical angle of internal fin,°
θ	apex of internal fin,°
λ	thermal conductivity, W/m K
ΔT_m	logarithmic mean temperature difference, K

Subscript

c	condensing
b	boiling
i	inside of tube
in	inlet of tube
ip	inside of plain tube
l	liquid
o	outside of tube
out	outlet of tube
p	plain
s	saturation
w	wall

enhancement ratio was decreasing. The next was Gewa-SE. Enhancement ratios ranged from 3.4 to 2.4. The heat transfer coefficient of Gewa-K26 and Gewa-TX19 were very close. Enhancement ratio was from 1.5 to 2.3. Investigations were also performed with refrigerants R22, R134a, R125 and R32 on low-fin, Turbo-B and Thermoexcel-E tubes by Jung et al. [9]. The heat flux was in the range of 10–80 kW/m^2. Heat transfer enhancement ratios of the low-fin and Turbo-B tubes were 1.09–1.68, 1.77–5.41, and 1.64–8.77, respectively. Thermoexcel-E showed the highest heat transfer coefficients in their experiments.

Pool boiling experiment of two tubes, Turbo-B5 and Gewa-B5, were performed by Rooyen and Thome [13]. The refrigerant included R134a, R236fa and R1234ze (E). Wilson plot method was used to determine the tube side heat transfer coefficient. Saturation temperature was from 5 to 25 °C, and heat flux ranged from 15 to 70 kW/m^2. Heat transfer results of R236fa were lower than R134a while R1234ze (E) performed similar to R134a. The heat transfer coefficients of R134a for Turbo-B5 were 26.2–28.6 kW/m^2K at the heat flux from 20 to 50 kW/m^2 and saturation temperature of 5 °C. At lower heat flux less than 40 kW/m^2, Gewa-B5 had 13%–19% higher heat transfer coefficient than Turbo-B5. While at the higher heat flux, Gewa-B5 has lower heat transfer coefficient than Turbo-B5.

In addition, many experiments have also been conducted in testing the condensing heat transfer of enhanced surfaces. Thermoexcel-C [7], Turbo-C [14–16], and Gewa-C [17] are some typical three-dimensional heat transfer tubes in condensation. Three-dimensional surfaces are developed based on the low-fin tube. The condensation on single smooth and low-fin tubes have been studied analytically [18–20]. However, general predictions are not yet available for three dimensional tubes.

Thome et al. [21–24] tested the condensing heat transfer of R134a and R234a on low-fin and three-dimensional enhanced tube Turbo-CSL and Gewa-C. Low-fin tube had a standard 26 fpi. The heat fluxes in the paper were 20, 40, and 60 kW/m^2. From the experiment, three-dimensional enhanced structures substantially outperformed low-fin tube. Higher enhanced heat transfer ratios of 13.4–16.8 were obtained for Gewa-C and Turbo-CSL. Gebauer et al. [25] tested the condensing heat transfer of R134a and propane on plain and finned tubes. The finned tubes included a low-fin tube with fin density 40 fpi and a three dimensional enhanced tube. Experiments were also performed on the two enhanced tubes with surface coatings of plasma polymer layer. At saturation temperature 37 °C, the heat flux varied from 4 kW/m^2 to 24 kW/m^2. The highest condensation heat transfer coefficients were observed on the uncoated three dimensional tube. At a heat flux of about 67.2 kW/m^2, the condensation heat transfer coefficient of the three dimensional tube was 1.8 times higher than low-fin tube. Both coated finned tubes showed lower heat transfer coefficient than uncoated tubes.

Recently, condensation heat transfer coefficients of R134a and R1234yf on a plain, low fin, and Turbo-C tubes were measured by Park et al. [26]. Low-fin tube had a standard fin density of 26 fpi. The effective heat transfer length was 0.29 m. All the data were taken at the saturation temperature of 39 °C with wall subcooling in the range of 3–8 °C. The measurements showed that the condensation heat transfer performance of R1234yf and R134a were quite close for all three tubes, the difference of which were even within ±1% in the test range.

Typically, the efficiency of enhancement profile is strongly dependent on the heat transfer mode. It is interesting to note that for the in-tube condensation of heat-pump, the tube that performs best for evaporation also performs best for condensation. The same enhanced profile of cross grooved tubes found to be effective in evaporation were also found to give remarkable heat transfer coefficient in condensation [27]. How about the film condensing tube performs in pool boiling and the boiling tube in condensing. The reports about the fundamentals is still limited to the author's knowledge. In order to further understand this process, the objective of this paper is trying to find that whether the tube with high performance in boiling is also found to be effective in condensing. It may help to further reveal the mechanisms of phase-change heat transfer and benefit to simplify the system by using the same enhanced tube in both condensing and boiling heat exchangers.

In this paper, heat transfer performance of four copper tubes is experimentally tested in both condensation and pool boiling. The

tubes include plain, integral-fin, and two commercial enhanced tubes No. 1 and No. 2. Integral-fin has the external fin number of 32 fpi. Pyramids-finned surface (No. 1) was made by making cross cuts through the integral fins. It is designed to take full advantage of the Gregorig effect [28]. The fins of re-entrant cavity surface (No. 2) are low and thick, with notches carving on the top of fins while the surface is rather flat compared with No. 1. The tubes used here have very typical profiles for shell and tube condenser and flooded evaporator of HVAC systems. Literature survey on the measurements of nucleate pool boiling and filmwise condensation is also conducted and compared with the experimental data.

The rest of the paper is organized as follows. In Section 2, experimental apparatus is introduced, including the circulating loop, specifications of test section and geometries of the tested tubes. Test procedure is presented in the third section. Section 4 provides the method of data reduction and the uncertainty analysis. The results and discussion are provided in Section 5. Finally some conclusions are summarized in Section 6

2. Experimental apparatus

The experimental apparatus includes three circulating loops: refrigerants, heating and cooling water. The schematic figure is shown in Fig. 1. The refrigerant circulating system includes evaporator, condenser, and ducts connecting the two vessels. The inner diameter of boiler is 257 mm, with length of 1100 mm. Internal diameter of condenser is 147 mm, which has the length of 1800 mm. The whole apparatus is well insulated with rubber material of thickness 40 mm and one layer of aluminum foil is used to enwrap the rubber.

When testing the heat transfer performances of tube in pool boiling, heating water is flowing through the inside of test tube and refrigerant is boiling outside. In vaporizing, refrigerant rises upward to the condenser through the duct connecting the evaporator and condenser. When the vapor reaches the condenser, it is condensed outside the tube fixed in the condenser. The cooling water is flowing through the tubes fixed in the condenser. After condensed, liquid refrigerant returns to the evaporator vessel by gravity. The heating water circulates through the tested tube and gets back to the water tank by a pump.

When testing the heat transfer coefficients of condensing tubes, the test procedure is similar, while the difference is only dependent on the measurement purpose. A metal sheet specially fabricated with a large number of small holes is mounted in the top of the condenser shell to distribute vapor uniformly along the condensing test tube.

Two pressure gauges are used to measure the pressures of the evaporator and condenser vessel. The measurement range is 2.5 MPa with precision of ±0.00625 MPa. Flow rates of cooling and heating water are measured by the weight-time flow meter. The temperature of refrigerant in different part of the system is measured by five platinum temperature transducer (with a precision of $\pm 0.15 + 0.002|T|$K at the test range). The difference between inlet and outlet water's temperature of heating and cooling is measured by a six-junction copper-constantan thermocouple pile. Thermocouples are used to test the temperatures of inlet and outlet of heating and cooling water. The thermocouples and thermocouple piles were calibrated against a temperature calibrator which had the precision of ±0.2 K. A Keithley digital voltmeter having the resolution of 0.1 μV is used to measure the electric potential of transducer.

The specifications of four tubes are given in Table 1. The geometries of enhanced tubes are shown in Fig. 2. d_o is the diameter of the embryo tube. The test length of boiling is 1100 mm and condensing is 1800 mm. No. 1 is designed for condensing with pyramids profiles. It is manufactured through an additional machining process applied to a low fin tube. The transformation machining process based on the helical fins with toothed wheel-like disc tool is used to obtain the pyramid surface. The pyramids outside the tube are approximately helically arranged and located side by side. The fins of No. 2 are flattened based on integral-fin with connecting tunnels under the surface. It has circumferential and axial grooves on the outer surface by a roll forming process. Circumferential grooves open to the refrigerant and have opening space. The width of which is narrower than that of bottom. The axial grooves have the depth shallower than the circumferential grooves, which are

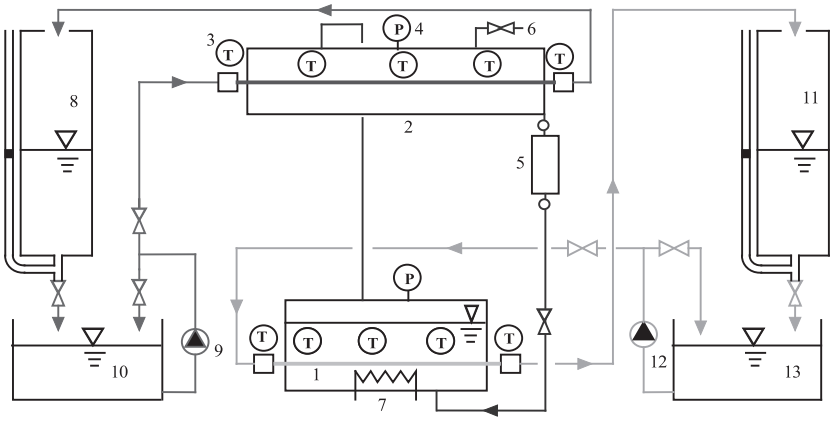

(1)Evaporator;(2)condenser;(3)thermocouple;(4)pressure gauge;(5)condensate measuring container;(6)exhausting valve;(7)subsidiary electric heater;(8)weight-time flow meter of cooling water;(9)cooling water pump;(10)cold water storage tank; (11) weight-time flow meter of heating water; (12)heating water pump; (13)hot water storage tank.

Fig. 1. Schematic diagram of the experimental apparatus.

Table 1
Specifications of test tubes.

Tubes	Outside diameter d_o(mm)	Inside diameter d_i(mm)	Height of inside fin H(mm)	Apex of internal fin θ(°)	Helical angle of internal fin α(°)	Internal starts number	Height of outside fin e(mm)	Outside fins per inch
Plain	19.09	16.41	–	–	–	–	–	–
Integral-fin	19.06	16.28	–	–	–	–	1.40	32
No. 1	18.78	14.53	0.33	131	34	20	0.86	35
No. 2	18.50	15.07	0.40	62	38	45	0.63	40

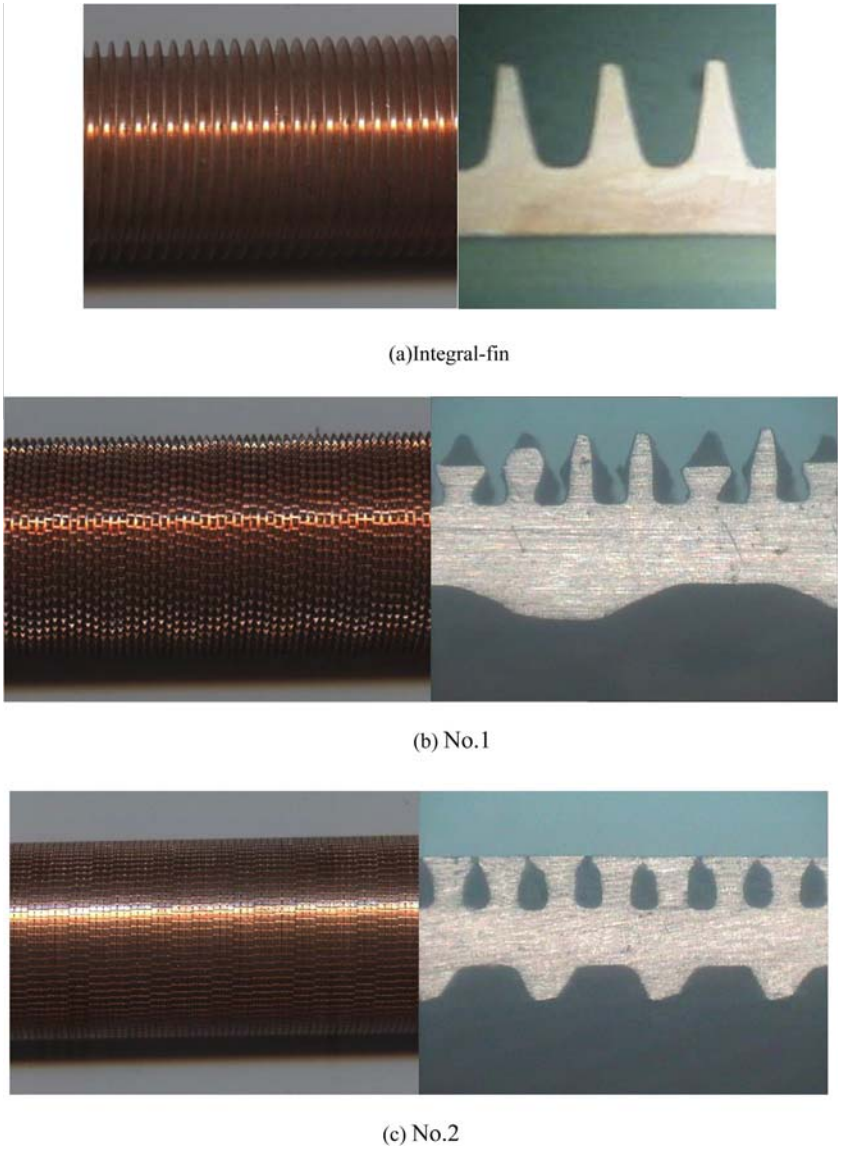

Fig. 2. Geometries of enhanced tubes.

used to connect opening spaces of adjacent circumferential grooves to each other. The refrigerant is brought into contact with the outer surface by the grooves. It should be emphasized that test sections used in pool boiling and condensing for the same profile were cut from the same tube.

3. Experimental procedures

Firstly, the tubes were fixed in boiler and condenser vessels. The whole system was charged with high pressure nitrogen, nearly 1.2 MPa, 1.2 times of the saturate pressure of R134a at 40 °C. Tightness-check was then performed to ensure the whole system was well sealed at this pressure. This pressure should be kept at least 24 h and no leakage should be detected. Before refrigerant was charged in, the whole system was evacuated to an absolute pressure of less than 800 Pa. Small amount of refrigerant was firstly charged into the boiler, and then evacuate. Repeat this process at least three times, until the content of other gas was reduced to a minimal level. Finally, refrigerant was charged into the evaporator until the level was up to at least 20 mm above the boiling tubes.

In the experiment, the amount of the non condensing gas was checked by two temperatures: one was measured from

temperature probe and the other was got from the measured pressure in the vessel according to thermodynamic properties of NIST [29]. The widely acceptable difference between these two temperatures was 0.2 K [30,31]. If not, the discharge process from the valves in two end of condenser should be repeated to meet this requirement.

Steady state measurements were made after the system had operated at least 3 h. The steady state was characterized by the fact that temperatures of refrigerant and water were in the required scope for at least twenty minutes. The inlet temperature of water, water flow rate and saturate temperature of refrigerant were maintained constant. The experiment was conducted at a steady state, but the absolute steady state is difficult to acquire in practice. Some fluctuation might still exist. The allowed inlet and outlet temperature fluctuation of water was within 0.1 K, and refrigerant was 0.05 K (Directly monitored results). This fluctuation might be caused by the temperature difference inside the water storage tank; Or heating and cooling inside the water storage tank. Water flow rate was within ±0.1 m/s. The experiment result is the average of a set of data contains 10 observations lasted for 5 min. Data of experimental measurements in pool boiling and condensing for No. 2 are shown in Table 2.

The water flow rate inside the test tubes is in the range of 0.97–2.58 m^3/h. Heat transfer rate for boiling tube is in the range of 617–4989 W and condensing is 982–9134 W. The inlet temperature of boiling tubes is in the range of 7.2–13.4 °C and condensing tube is 18.5–38.4 °C. The outlet temperature is dependent on the heat flux and water flow rate.

The boiling and condensing experiments are investigated separately. When the tube in the boiler is tested for boiling, the tube in condenser is used to condense the vaporized refrigerant. In condensing experiment, the tube in boiler provides the vapor for condensing measurements.

4. Data reduction and analysis of uncertainties

The heat balance is firstly examined by power inputs and outputs.

Heating power inputs by heating water:

$$\phi_b = m_b c_p (T_{b,1} - T_{b,2}) \tag{1}$$

Cooling power outputs by cooling water:

$$\phi_c = m_c c_p (T_{c,2} - T_{c,1}) \tag{2}$$

where, $T_{b,1}$, $T_{b,2}$ are the inlet and outlet temperatures of heating water (K). $T_{c,1}$, $T_{c,2}$ are the inlet and outlet temperatures of cooling water (K). c_p is the specific heat capacity of water corresponding to the mean temperature of inlet and outlet water (J/kg K). m_b and m_c are the mass flow rates of heating and cooling water (kg/s). The properties of water is obtained from [6].

The maximum differences between two heat transfer rates are within 3%. The average of the two heat transfer rates, ϕ, is used to determine the overall heat transfer coefficient.

The overall heat transfer coefficient is calculated using the following equation:

$$k = \frac{\phi}{A_o \cdot \Delta T_m} \tag{3}$$

The heat transfer surface area A_o is based on the outside diameter of embryo tube, calculated by $A_o = \pi d_o L$. L is the length of test section. Heat flux is calculated by $q = \phi/A_o$. It should be noted that the heat flux is average value, not local measurements. The heat flux might be decreasing along the flow inside the tube.

ΔT_m is the log-mean temperature difference:

$$\Delta T_m = \frac{T_{b,1} - T_{b,2}}{\ln \frac{T_s - T_{b,2}}{T_s - T_{b,1}}} \text{ in pool boiling} \tag{4}$$

$$\Delta T_m = \frac{T_{c,2} - T_{c,1}}{\ln \frac{T_s - T_{c,1}}{T_s - T_{c,2}}} \text{ in condensing} \tag{5}$$

Where T_s is the saturate temperature of refrigerant. The boiling and condensing heat transfer coefficient for the test tubes is obtained by subtracting the thermal resistance of water in tube side, wall and fouling from overall thermal resistance.

$$\frac{1}{h_o} = \frac{1}{k} - \frac{A_o}{A_i}\frac{1}{h_i} - R_f - R_w \tag{6}$$

Where R_f is the thermal resistance of foul. It is neglected because either internal or outer surface has been cleaned using acetone solution and the running time of apparatus for one tube is one week at most. R_w is the thermal resistance of the wall. A_i is the area of inside tube. h_o is the heat transfer coefficients of boiling or condensing. h_i is heat transfer coefficient of water side.

When the inside of test tube is smooth, the water side heat transfer coefficient can be calculated using Gnielinski correlation [32]:

$$h_{ip} = \frac{\lambda}{d_i}\frac{(f/8)(\mathrm{Re} - 1000)\mathrm{Pr}}{1 + 12.7(f/8)^{1/2}(\mathrm{Pr}^{2/3} - 1)}\left[1 + \left(\frac{d_i}{L}\right)^{2/3}\right]\left(\frac{\mathrm{Pr}}{\mathrm{Pr}_w}\right)^{0.11} \quad (\mathrm{Re}: 2300 - 10^6, \mathrm{Pr}: 0.6 - 10^5) \tag{7}$$

In experiment, Re of water is in the range of 10,000–90,000 corresponding to the water velocity of 1.5–4.0 m/s. If the internal surface is enhanced with helical grooves, Wilson plot technique is used to obtain the heat transfer coefficients of water side [30], which is introduced in detail by Rose [35]. For integrity, the method is presented here briefly. When the saturation temperature of refrigerant and heat flux is maintained relatively constant, h_o should approach a specific value. Then the equation of (6) changes into:

$$\frac{1}{k} = a\frac{1}{h_{ip}} + b \tag{8}$$

In this equation,

$$a = \frac{d_o}{d_i}\frac{1}{c_i} \tag{9}$$

$$b = \frac{1}{h_o} + R_w \tag{10}$$

where: $R_w = 0.5 d_o \ln(d_o/d_i)/\lambda$.

In experiment, the heat flux is fixed and a group of data are obtained. The slope of fitting line, and the enhanced ratio of water side, c_i, compared with plain tube, should be obtained. By doing so, we would get the inside and outside heat transfer coefficients. Figure 3 is the Wilson plots for two internal enhanced tubes in pool boiling. The enhance ratios for No. 1 and No. 2 are 1.9 and 3.0 respectively.

An uncertainty analysis according to literature [30,36] has been adopted to estimate the possible uncertainty of experimental

Table 2
Data of measurements in pool boiling and condensing for No. 2.

Tubes	Pool boiling	Condensing
Water velocity (m/s)	2.0	2.0
$T_{in}/T_{out}/T_s$(°C)	35.8/37.6/40	3.7/5.6/6
Heat flux (W/m^2)	30967	30493
h_{in}(W/m^2K)	23859.6	22889.6
h_o(W/m^2K)	21284.9	17545.4

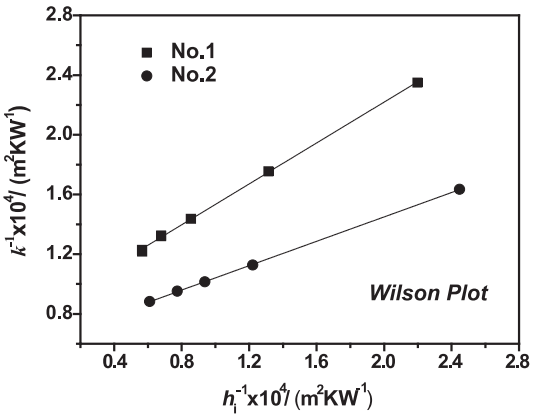

Fig. 3. Wilson plots of internal enhanced tubes.

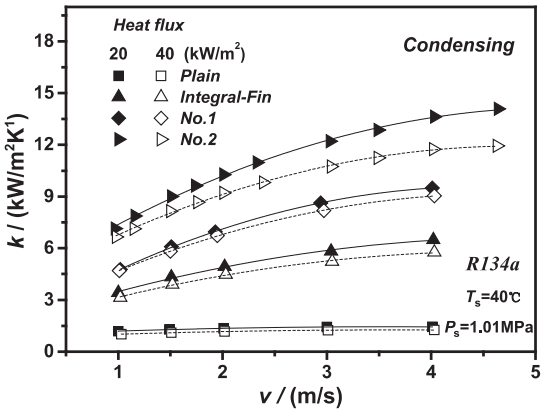

Fig. 5. Overall heat transfer coefficient versus water velocity in condensing.

results. In boiling, for plain, integral-fin, No. 1, and No. 2, the estimated uncertainties of k are less than 6.8%, 5.3%, 5.7%, and 5.4%, respectively. As h_o is not directly measured, the uncertainties of h_o is estimated using the following method. To calculate h_o, which involved k, h_i and the thermal resistance of tube wall R_w, the uncertainties in calculation h_i is considered of 10% [32–34]. The worst situation calculating h_o occurred as the overall thermal resistance and that of water side thermal resistance are happened to be in an opposite direction. For example, the overall thermal resistance is in a positive direction, and that of water side is in a negative direction. Under such circumstance a maximum error of h_o occurs. Therefore, the uncertainties are in the range of 13.8%–25.5%, 19.4%–32.2%, 18.3%–28.4%, and 20.6%–34.1% for plain, integral-fin, No. 1, and No. 2 respectively. The uncertainties of four tubes in condensing are analyzed with the same method. For plain, integral-fin, No. 1, and No. 2, their estimated uncertainties of h_o are respectively of 9.9%–18.7%, 13.3%–33.5%, 13.0%–30.4%, and 11.2%–32.8%.

5. Results and discussion

5.1. Overall heat transfer coefficients

Figures 4 and 5 show the dependence of overall heat transfer coefficients on internal water velocity. The saturate temperature is 6 °C in pool boiling and 40 °C in condensing. The velocity ranges from 1.0 to 4.6 m/s. The heat flux is maintaining at 20 and 40 kW/m^2. As shown in the figures, the following features can be observed.

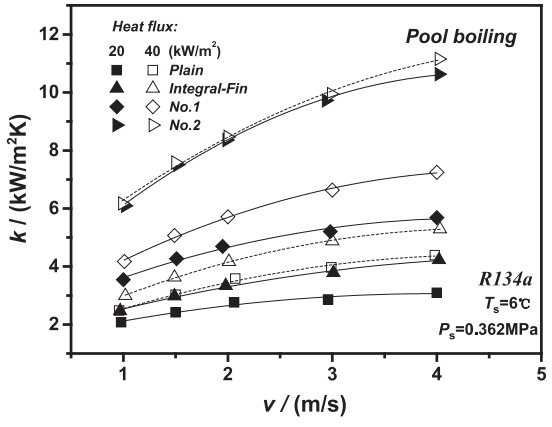

Fig. 4. Overall heat transfer coefficient versus water velocity in pool boiling.

(1) Integral-fin and tube No. 1 have moderate overall heat transfer performance both in pool boiling and condensing. One of the reasons is that the internal surface of integral-fin tube is smooth and tube side enhanced ratio of No. 1 is very low. It is also found that the overall heat transfer coefficient for three enhanced tubes in condensing is higher than boiling at the same water velocity. The overall heat transfer coefficient of integral-fin tube in condensing is 38.5%–53.5% higher than boiling at the heat flux 20 kW/m^2. However, for the plain tube, the pool boiling overall heat transfer coefficient is higher than condensing. It is chiefly due to the external phase-change heat transfer coefficient and heat flux.

(2) For No. 2, it has the highest overall heat transfer performance in either condensing or boiling. The heat transfer coefficients of No. 2 are 6.0–9.5 and 2.9–3.4 times over plain tube in condensing and boiling respectively. As mentioned earlier, No. 2 is designed for pool boiling with cavity profiles in the surface; however, the heat transfer of condensing is also substantially improved. It gives equivalent overall heat transfer coefficient with Gewa-C in [37] in condensing.

(3) At water velocity of 2.0 m/s in condensing, for No. 2, the ratio of thermal resistance for tube and shell side is 52.3% and 42.8% respectively at heat flux of 20 kW/m^2; it is 45.7% and 50.3% in boiling. It is generally in the same order of magnitude. For condensation at heat flux 20 kW/m^2, further enhancement of vapor side seems to have less effect than water side, because the thermal resistance of water coolant in the tube side is higher.

5.2. Heat transfer in boiling and condensing

5.2.1. Plain tube

The heat transfer coefficients of plain tube in pool boiling is firstly compared with Cooper equation [38]. Cooper equation is given by:

$$h_o = Cq^{0.67}Mr^{-0.5}P_r^m(-lgP_r)^{-0.55} \quad (11)$$

where: $C = 90W^{0.33}/(m^{0.66}\cdot K)$, $m = 0.12 - 0.2\lg\{R_p\}_{\mu m}$.

Figure 6 shows the comparison of experimental result with Cooper equation. h_o is calculated under the same experimental condition. R_p used here is 0.3 μm suggested by [38] for commercial plain tubes. The relative difference between Cooper and experimental result is from 2.4% to 9.1%. The comparison should also confirm the reliability of experimental data for other tubes.

The experimental result of plain tube in film condensing is also compared with Nusselt analytical solution [39]. The expression of

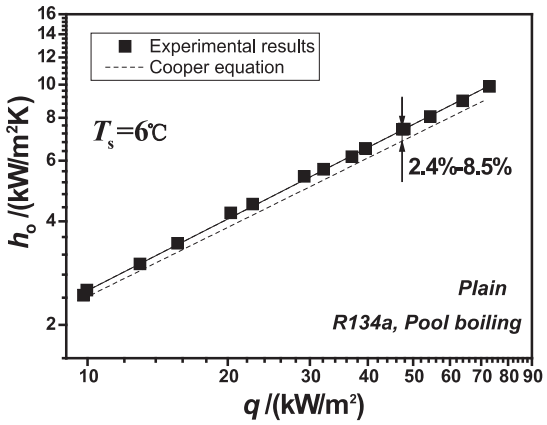

Fig. 6. Comparison of experiment result with Cooper equation.

Nusselt analytical solution for condensation on single horizontal tube is written as:

$$h_p = 0.729\left(\frac{rg\lambda_l^3\rho_l^2}{\mu_l d_o(t_s - t_w)}\right)^{1/4} = 0.656\left(\frac{rg\lambda_l^3\rho_l^2}{\mu_l d_o q}\right)^{1/3} \quad (12)$$

Figure 7 shows the comparison of the experimental result with Nusselt analytical solution. The relative deviation of experimental result from Nusselt analytical solution is within ±15%.

5.2.2. Enhanced tube in pool boiling

Pool boiling heat transfer performances were tested at the saturation temperature of 6 °C. Experimental data are presented in Fig. 8 in the forms of pool boiling heat transfer coefficient versus heat flux. The range of heat flux is from 9 to 86 kW/m^2.

As shown in Fig. 8, the heat transfer coefficient of plain, integral-fin and No. 1 increases almost linearly with the increment of heat flux. Examination of the data show that the slopes of h_o versus q for integral-fin and No. 1 are 0.58 and 0.46 respectively. It is 0.67 for plain tube according to Cooper equation. The heat transfer coefficient might increase as the increment of fin height for integral-fin and No. 1. The model presented by Chien and Webb [40] is used to predict the heat flux of tube No. 2. The result is shown in Fig. 9. The deviation of experiment result from the model is from 14.9% to 69.9%.

Boiling heat transfer coefficients of No. 2 are higher than other three tubes. The slopes of boiling heat transfer coefficient versus heat flux curve are found to be heat flux dependent. It should be noted that according to the equation of Lienhard *et al.* [41], at the saturation temperatures of 6 °C, the reference critical heat flux for refrigerant R134a is 412.2 kW/m^2. The heat flux in the present investigation is less than the critical heat flux. Compared with plain tube, the enhanced ratio is 4.9–1.8, which is decreasing as the increment of heat flux. A significant improvement is observed at lower heat flux. The increasing trend of heat transfer coefficients is gradually becoming mild as the increment of heat flux. At higher heat flux greater than 20 kW/m^2, the heat transfer coefficients of No. 2 are almost independent of heat flux and maintains relatively invariant. For No. 2, the probable physics of enhanced heat transfer is thin film evaporation occurs over a large surface area inside the cavity, the cavities might be full of vapor and easy to be agitate for nucleation. When the bubble is ejected through the opening of cavity. The liquid is sucked into the tunnel space through inactive pores by the pumping action of bubbles growing at active pores. This liquid is warmed up when flows through the narrow gap and reach the necessary superheat level required for nucleation. The period of bubble generation and departure is decreased. For the smooth tubes, reliable nucleation sites on plain surfaces is not easily accomplished and the number is limited. As a bubble leaves the nucleation sites, the fully exposed nucleation sites might be filled with sub-cooled refrigerant and the cycle for boiling is elongated. A relatively large heat flux is required to bring this cold liquid to the incipient boiling point. For the low-fin and tube No. 1,

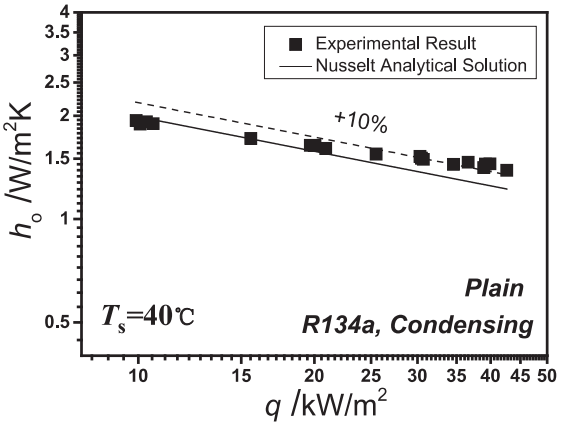

Fig. 7. Comparison of experiment result with Nusselt analytical solution.

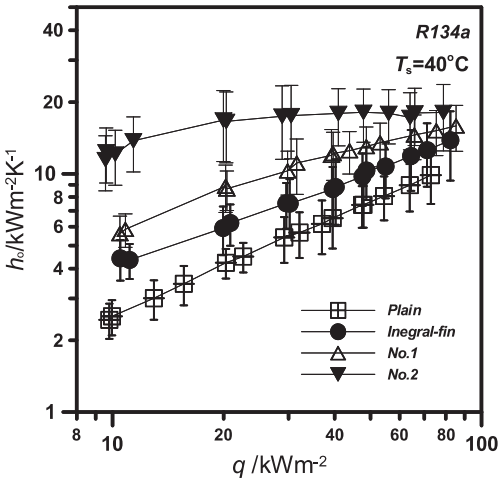

Fig. 8. Pool boiling heat transfer coefficient of four tubes.

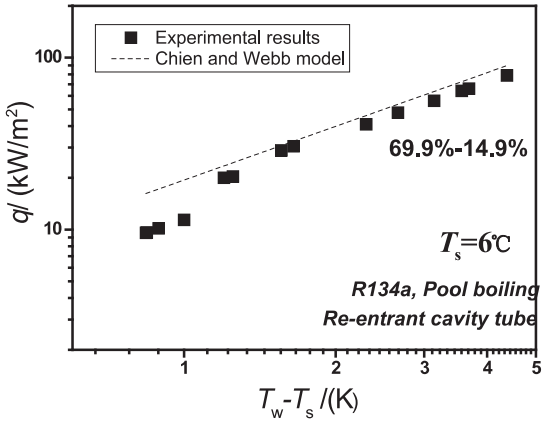

Fig. 9. Comparison of pool boiling experiment result and Chien and Webb model for No.2.

enhanced heat transfer is mostly accomplished simply by area increase [42–44]. The heat transfer coefficients are quite close for No. 1, No. 2 and integral-fin tubes at the higher heat flux greater than 70 kW/m^2.

Figure 10 is the comparison of present results with other literature measurements. Refrigerant for comparison is R134a and the saturation temperature is in the range of 0–10 °C. Twelve tubes like Gewa-K26, Gewa-TX19, Gewa-SE, Turbo-B, Turbo-BII HP, and Turbo-CSL obtained by Webb and Pais [8], Wang et al. [45], Kim and Choi [46], Jung et al. [9], Ribatski and Thome [12], and Rooyen and Thome [13] are presented. Thermoexcel-E and latest generation Wieland Gewa-B5 tube provide the highest heat transfer coefficient. Gewa-B, Turbo-B, the present tube No. 2 and re-entrant cavity surface falls into the second level, still very high. As shown in Fig. 10, the features for different evaporator tube geometry are as follows: firstly, for No. 2, the substantial heat transfer improvement is achieved at comparably lower heat flux, reaching a maximum at the heat flux around 30 kW/m^2, like Thermoexcel-E, Turbo-B and Gewa-B series. After the maximum, it follows by a stable heat transfer rate or even a gradual decrease. Further increment of heat flux has less effect on the heat transfer coefficient. Secondly, it is interesting to note that some tube like plain, integral-fin, open mouth surface like No. 1, and Turbo-CSL, the heat transfer performance is strongly dependent on heat flux. More nucleate sites can be activated as the increasing of heat flux. It results in rather modest augmentation in heat transfer at the lower heat flux. Higher heat transfer coefficient can only be observed at higher heat flux. Thirdly, at the higher heat flux, when a large quantity of bubbles are generated, heat transfer coefficients of all the tubes are quite close. Some tubes with very open mouth or grooves can even overtake the re-entrant tube, like Turbo-CSL, which is originally designed as condensing surface. The results indicate that the condensing tube Turbo-CSL outperforms Turbo-BII HP at heat flux greater than about 50 kW/m^2, whereas, at the lower heat flux, the heat transfer coefficients are much less than Turbo-BII HP.

In general, the tubes with different heat transfer features can be classified into two groups. First is the tube with re-entrant cavity structures, such as Thermoexcel-E, Gewa-B, Turbo-B and the present tube re-entrant cavity surface. Their heat transfer coefficients are rather high at low heat flux but cease to increase at high heat flux. Second is the tube with open mouth like No. 1, Turbo-CSL, Turbo-TX19 and integral-fin tubes. A linear increment of heat transfer coefficient is observed as the increment of heat flux for the second group of tubes.

5.2.3. Enhanced tube in condensing

Figure 11(a) shows the dependence of condensing heat transfer coefficients on heat flux for the same four tubes. The condensing saturation temperature of the system is maintained at 40 °C. Heat flux ranges from 8 to 100 kW/m^2. As depicted in Fig. 11(a), the following features can be observed:

For the integral-tube, it has lower heat transfer coefficients compared with the other two enhanced tube. The enhanced ratios are in the range of 5.7–6.6. The condensing experimental result of integral-fin tube is also compared with prediction of the Beatty–Katz [47], Owen [48], Honda [18], Webb [49], Rose [20] and Briggs–Rose [50]. The apex angle of fin is 23°. Fin height and pitch are 1.4 mm and 1.24 mm respectively. Figure 11(b) shows the comparison of condensation heat transfer coefficient of R134a with that predicted by theoretical models. It is found that Beatty and

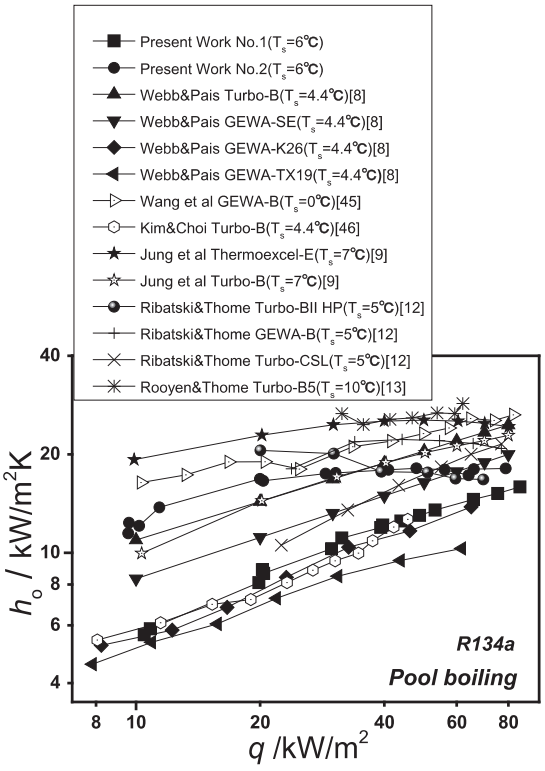

Fig. 10. Comparison of experimental data with other measurements in pool boiling.

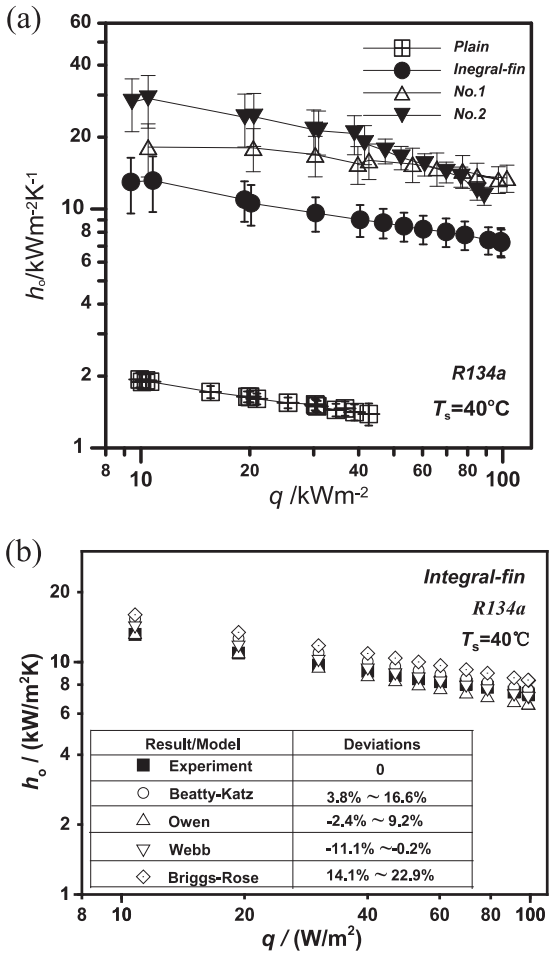

Fig. 11. (a) Condensing heat transfer coefficient of four tubes. (b) Comparisons of experiment result with prediction models for integral-fin tube.

Katz model, based on the assumption of gravity drainage on either the fin or base surface of the tubes, over-predicts the experimental results within 3.8%–16.6%. The predictions difference of Owen and Webb models are approximately within ±10%. Over-predictions in a range of 14.1%–22.9% are observed with Briggs–Rose model. The deviations of Honda model are generally in the range of −52%∼68.3%, and over-predictions of 28.8%–44.6% are found for Rose model. Taking into account the experimental uncertainty, the present experimental data agrees better with the models of Beatty–Katz, Owen–Webb, and Briggs–Rose. However, it does not mean that these three models have the highest degrees of accuracy; because it is also dependent on the experimental conditions.

The condensing heat transfer coefficient of No. 1 is 1.4–1.9 times higher than integral-fin tube. The fins of No. 1 is designed like a pyramid as mentioned above, and the bottom of the tower may thinner than the middle. This kind of design is going to take full advantage of "Gregorig effect", whereby condensation occurs mainly at the tops of convex ridges. This effect is gradually enhanced as the increment of heat flux and condensate thickness. The heat transfer coefficient of No. 1 overtakes No. 2 at the heat flux of 63 kW/m^2. Examination of Fig. 11(a) also shows that the decreasing rate of No. 1 is obviously lower than integral-fin and No. 2. Lower percentage of decreasing rate in heat transfer coefficient is observed. The decreasing ratio is 20.4% for No. 1, while it is 54.9% for No. 2 as the heat flux increasing from 10 to 77 kW/m^2.

No. 2 has the highest heat transfer coefficient at the lower heat flux less than 63 kW/m^2. The surface is compactly distributed square blocks. Gewa-TWX tube in the paper of Chang et al. [37], with similar profile as No. 2, originally developed as evaporator tubes, is also found to give superior heat transfer performance in condensation. The spacing of fins is 1.337 mm, only 19 fpi; fin height is 0.95 mm. However, the heat transfer coefficient is quite close to the integral-fin tube which has external fin density of even 40 fpi and fin height of 1.26 mm.

Data from literature are also compared with present work in Fig. 12. Refrigerant for comparison is R134a and the saturation temperature ranges from 31 to 40.6 °C. Ten tubes including Gewa-C, Gewa-TWX, Pyramid surface tube, Turbo-Chil, Turbo-C, Turbo-CSL and Thermoexcel-C from the measurements of Chang et al. [37], Mitrovic [51], Belghazi et al. [52,53], Zhang et al. [54], Gstoehl and Thome [21], and Park et al. [26] are compared. As shown in Fig. 12, the main features can be summarized as follows: (1) At lower heat flux less than 30 kW/m^2, the heat transfer coefficients of No. 2 and Gewa-C are quite close and No. 2 is even a little bit higher than other enhanced profiles. Three Gewa-C tubes, Thermoexcel-C, and Tuobo-CSL belong to the first group with highest heat transfer performance at higher heat flux. Tubo-Chil, two pyramid-surface tubes fall into the second level. (2) The heat transfer coefficient of all the tubes are decreasing with the increment of heat flux, while the decreasing rate of No. 2 is apparently higher than the other tubes. The evaporator tube Gewa-TWX mentioned earlier designed for pool boiling has almost the same decreasing rate with No. 2 at higher heat flux. (3) Despite the value of heat transfer coefficient is relatively small, No. 1 has similar decreasing ratios as Thermoexcel, Gewa and Turbo tube series. By a non-linear fitting of the heat transfer coefficients with equation $h_o = a \cdot q^b$, the index b of No. 1 and No. 2 are respectively of −0.12 and −0.38. The tube used in the experiment of Mitrovic [55] has similar shape with No. 1. Very similar heat transfer performance is also observed.

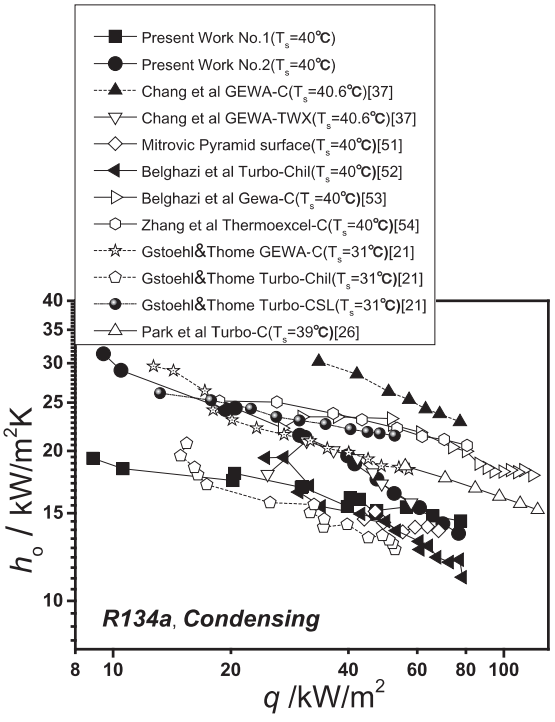

Fig. 12. Comparison of experimental data with other measurements in condensing.

Furthermore, as shown in Figs. 8–10 and 12, it should be note that the condensing heat transfer coefficient of plain tube is lower than pool boiling in the test range. However, the highest enhanced ratio of the tube in literature for pool boiling is 2.5–7.9 and condensing is 13.2–23.1 in the heat flux of 8–100 kW/m^2. The condensing heat transfer coefficient of the enhanced tubes is obviously higher than nucleate pool boiling. It may indicate that it is still possible for the further intensification of pool boiling heat transfer.

Now attention is turned to the analysis why No. 2 has higher heat transfer performance in either pool boiling or condensing. As No. 2 is designed for pool boiling, it is not surprising that higher heat transfer coefficient is obtained in boiling. In film condensing, two major forces acting on liquid film are gravity and surface tension. The surface tension may dominate to draw the liquid from tips of fin to the root. Grooves between fins may collect condensate from the top area. As depicted in Fig. 2, surface tension on the structure of No. 2 could also play an important role in pulling the condensate easily from small and tight evenly distributed rectangular blocks, where it run off easily. The relatively flat surface and special arrangement of blocks gives superior performance in reducing the thickness of condensate at lower condensing rate. While the surface of three dimensional tube like No. 1 may hold and keep condensate over the complicate structures with small sharp tips at lower heat flux, which would affect the heat transfer performance at lower heat flux. However, at higher heat flux with more condensate in the fin surface, Grigorig effect plays an important role in drawing liquid from the micro-fin tips towards their root, whereby condensation occurs mainly at the tops of sharp rigs. Tubes like No. 2 have small fin height, with very weak Grigorig effect. The average film thickness of No. 2 is thicker than the profile like Gewa-C, so the decreasing rate is higher than 3-D structures. That's why this tube had lower performance in condensing at higher heat flux more than 63 kW/m^2.

It should be noted that the external fin density of No. 2 is not the highest as that from literatures. Like Thermoexcel-E in Jung et al. [14], the fin density is 49 fpi. Turbo-BIII has even external fin density of 60 fpi [55]. Intensification of the structure based on No. 2 with more and long fins can probably further enhance the nucleate pool boiling heat transfer. In addition, the sharp fin tip and convex ridges designed for condensing have shortcomings, as it can be easily destroyed in transportation or insertion into a tube plate, but the profile designed like No. 2 can prevent it.

By comparison of the experiment result of No. 2, Turbo-TWX in [37], and Turbo-CSL in [12,21], the statement of Bergles [27] seems

still routinely valid for some enhanced profiles in nucleate pool boiling and filmwise condensation for a specific heat flux range. That is the tube of cross grooved tubes that performs best for evaporation can also be effective in condensation. Especially at lower heat flux less than 40 kW/m^2, it is in the normal range of HVAC heat exchangers. However, because the nucleate sites is not easily to be activated with the open structure at lower heat flux, the tubes gives superior performance in condensation seems not necessarily being effective in pool boiling, such as Turbo-CSL.

6. Conclusions

Pool boiling and film-wise condensation heat transfer performance of R134a on the same four horizontal copper tubes are investigated. The tubes include four typical profiles. Saturation temperature in the experiment is maintained at 6 and 40°C in pool boiling and condensing. The experiment results are also compared with the data in literature. From the data obtained by the present experiments and literature survey, the following conclusions can be drawn:

(1) Integral-fin tube with 32 fpi gives lowest heat transfer performance in the three enhanced tubes. In condensing, the deviations of heat transfer coefficient predicted by theoretical models of Owen or Webb and experiment result are within ±10%.
(2) It is found that No. 1 has higher heat transfer coefficient both in pool boiling and condensing at higher heat flux. With the increment of heat flux, the decreasing rate of heat transfer coefficient in condensing is lower than integral-fin tube and No. 2.
(3) Experiment results show No. 2 has rather superior overall and phase change heat transfer coefficient in both pool boiling and condensing, especially at higher heat flux less than 63 kW/m^2. The heat transfer coefficients can be 1.9–4.8 and 14.8–19.3 times those of a plain tube in pool boiling and condensing.
(4) Literature survey indicates some tubes of cross grooves that performs best for evaporation are also found to be effective in condensation. But the tube gives superior performance in condensation seems not necessarily being effective in pool boiling, especially at lower heat flux.

Acknowledgment

The supports from the National Key Basic Research Program of China (973 Program) (2013CB228304), NNSFC (51306140), SRFDP (20130201120057) and Daikin Cooperation of Japan are greatly acknowledged.

References

[1] F.P. Incropera, D.P. DeWitt, T.L. Bergman, A.S. Lavine, Fundamentals of Heat and Mass Transfer, John Wiley & Sons, 2011.
[2] J.H. Lienhard, A heat transfer textbook, Courier Dover Publications, Cambridge, Massachusetts, USA, 2011.
[3] A.E. Bergles, Recent developments in enhanced heat transfer, Heat Mass Transfer 47 (8) (2011) 1001–1008.
[4] A.E. Bergles, R.M. Manglik, Current progress and new developments in enhanced heat and mass transfer, J. Enhanced Heat Transfer 20 (1) (2013) 1–15.
[5] R.L. Webb, N.H. Kim, Principle of Enhanced Heat Transfer, second ed., Taylor & Francis, Boca Raton, 2005.
[6] S.M. Yang, W.Q. TAO, Heat Transfer, 4th ed., Higher Education Press, Beijing, 2006.
[7] W. Nakayama, T. Daikoku, H. Kuwahara, K. Kakizaki, High-flux heat transfer surface "THERMOEXCEL", Hitachi Rev. 24 (1975) 329–331.
[8] R.L. Webb, C. Pais, Nucleate pool boiling data for five refrigerants on plain, integral-fin and enhanced tube geometries, Int. J. Heat Mass Transfer 35 (8) (1992) 1893–1904.
[9] D. Jung, K. An, J. Park, Nucleate boiling heat transfer coefficients of HCFC22, HFC134a, HFC125, and HFC32 on various enhanced tubes, Int. J. Refrig. 27 (2) (2004) 202–206.
[10] Z.H. Ayub, A.E. Bergles, Pool boiling from GEWA surfaces in water and R-113, Heat Mass Transfer 21 (4) (1987) 209–219.
[11] R.K. Al-Dadah, T.G. Karayiannis, Passive enhancement of condensation heat transfer, Appl. Therm. Eng. 18 (9–10) (1998) 895–909.
[12] G. Ribatski, J.R. Thome, Nucleate boiling heat transfer of R134a on enhanced tubes, Appl. Therm. Eng. 26 (10) (2006) 1018–1031.
[13] E. Van Rooyen, J. Thome, Pool boiling data and prediction method for enhanced boiling tubes with R-134a, R-236fa and R-1234ze (E), Int. J. Refrig. 36 (2) (2013) 447–455.
[14] D. Jung, C.B. Kim, S.-M. Hwang, K.K. Kim, Condensation heat transfer coefficients of R22, R407C, and R410A on a horizontal plain, low fin, and turbo-C tubes, Int. J. Refrig. 26 (4) (2003) 485–491.
[15] D. Jung, S. Chae, D. Bae, G. Yoo, Condensation heat transfer coefficients of binary HFC mixtures on low fin and Turbo-C tubes, Int. J. Refrig. 28 (2) (2005) 212–217.
[16] Y.T. Kang, H. Hong, Y.S. Lee, Experimental correlation of falling film condensation on enhanced tubes with HFC134a; low-fin and Turbo-C tubes, In. J. Refrig. 30 (5) (2007) 805–811.
[17] M.B. Pate, Z.H. Ayub, J. Kohler, Heat exchangers for the air-conditioning and refrigeration industry: state-of-the-art design and technology, Heat Transfer Eng. 12 (3) (1991) 56–70.
[18] H. Honda, S. Nozu, A prediction method for heat transfer during film condensation on horizontal low integral-fin tubes, ASME J. Heat Transfer 109 (1) (1987) 218–225.
[19] H. Honda, S. Nozu, B. Uchima, A generalized prediction method for heat transfer during film condensation on horizontal low fin tube, in: ASME-JSME Therm. Eng. Joint Conference, 1987, pp. 385–392.
[20] J. Rose, An approximate equation for the vapour-side heat-transfer coefficient for condensation on low-finned tubes, Int. J. Heat Mass Transfer 37 (5) (1994) 865–875.
[21] D. Gstoehl, J. Thome, Film condensation of R-134a on tube arrays with plain and enhanced surfaces: Part I—experimental heat transfer coefficients, J. Heat Transfer 128 (1) (2006) 21–32.
[22] D. Gstoehl, J. Thome, Film Condensation of R-134a on Tube Arrays With Plain and Enhanced Surfaces: Part II—Empirical Prediction of Inundation Effects, J. Heat Transfer 128 (1) (2006) 33–43.
[23] M. Christians, M. Habert, J.R. Thome, Film condensation of R-134a and R-236fa, part 1: experimental results and predictive correlation for single-row condensation on enhanced tubes, Heat Transfer Eng. 31 (10) (2010) 799–808.
[24] M. Christians, M. Habert, J.R. Thome, Film condensation of R-134a and R-236fa, part 2: experimental results and predictive correlation for bundle condensation on enhanced tubes, Heat Transfer Eng. 31 (10) (2010) 809–820.
[25] T. Gebauer, A.R. Al-Badri, A. Gotterbarm, J.E. Hajal, A. Leipertz, A.P. Fröba, Condensation heat transfer on single horizontal smooth and finned tubes and tube bundles for R134a and propane, Int. J. Heat Mass Transfer 56 (1) (2013) 516–524.
[26] K.-J. Park, D.G. Kang, D. Jung, Condensation heat transfer coefficients of R1234yf on plain, low fin, and Turbo-C tubes, Int. J. Refrig. 34 (1) (2011) 317–321.
[27] A.E. Bergles (Enhanced heat transfer: endless frontier, or mature and routine?), in: Appl Optical Measurements, Springer, 1999, pp. 3–17.
[28] R. Gregorig, Film condensation on finely rippled surfaces with consideration of surface tension, Z. Angew. Math. Phys 5 (1954) 36–49.
[29] N.R.P.D. 23, REFPROP, in, NIST, Gaithersburg, MD, 1998.
[30] B. Cheng, W.Q. Tao, Experimental study of R-152a film condensation on single horizontal smooth tube and enhanced tubes, ASME J. Heat Transfer 116 (1) (1994) 266–270.
[31] W.-T. Ji, C.-Y. Zhao, D.-C. Zhang, Z.-Y. Li, Y.-L. He, W.-Q. Tao, Condensation of R134a outside single horizontal titanium, cupronickel (B10 and B30), stainless steel and copper tubes, Int. J. Heat Mass Transfer 77 (2014) 194–201.
[32] V. Gnielinski, New equations for heat and mass transfer in turbulent pipe and channel flows, Int. Chem. Eng. 16 (1976) 359–368.
[33] Yunus A. Cengel, Afshin J. Ghajar (Heat and Mass Transfer), Fourth ed., McGraw-Hill, New York, 2011. p. 489.
[34] Theodore L. Bergman, Adrinne S. Lavine, Frank P. Incropera, David P. DeWitt, Introduction to Heat Transfer, Sixth ed., John Wiley & Sons Inc, Hoboken, NJ, 2011.
[35] J.W. Rose (Heat-transfer coefficients, Wilson plots and accuracy of thermal measurements), Exp. Therm. Fluid Sci. 28 (2-3) (2004) 77–86.
[36] S.J. Kline, F.A. McClintock (Describing uncertainties in single-sample experiments), Mech. Eng. (1953) 3–8.
[37] Y.J. Chang, C. Hsu, C.C. Wang, Single-tube performance of condensation of R-134a on horizontal enhanced tubes, ASHRAE Trans. 102 (1) (1996) 821–829.
[38] M.G. Cooper, Saturation nucleate pool boiling-a simple correlation Int, Chem. Eng. Symp. Ser. 86 (1984) 785–792.
[39] W. Nusselt, Die oberflachencondensation des wasserdampfes, VDI 60 (1916) 541–569.
[40] L.-H. Chien, R.L. Webb, A nucleate boiling model for structured enhanced surfaces, Int. J. Heat Mass Transfer 41 (14) (1998) 2183–2195.

[41] J.H. Lienhard, V.K. Dhir, D.M. Riherd, Peak pool boiling heat-flux measurements on finite horizontal flat plates, J. Heat Transfer 95 (1973) 477.
[42] R.L. Webb, Heat transfer surface having a high boiling heat transfer coefficient, in, Google Patents, 1972.
[43] A.E. Bergles, High-flux processes through enhanced heat transfer, in: 5th International Conference on Boiling Heat Transfer, Montego Bay, Jamaica, 2003.
[44] R.L. Webb, Odyssey of the enhanced boiling surface, J. Heat Transfer 126 (6) (2004) 1051–1059.
[45] C.C. Wang, W. Shieh, Y. Chang, C. Yang (Nucleate boiling performance of R-22, R-123, R-134 a, R-410 A, and R-407 C on smooth and enhanced tubes), ASHRAE Trans. (1998) 1315–1321. SF-98-15-4.
[46] N.H. Kim, K.K. Choi, Nucleate pool boiling on structured enhanced tubes having pores with connecting gaps, Int. J. Heat Mass Transfer 44 (2001) 17–28.
[47] K.O. Beatty, D.L. Katz, Condensation of vapors on outside of finned tubes, Chem. Eng. Prog. 44 (1) (1948) 908–914.
[48] R.G. Owen, R.G. Sardesai, R.A. Smith, W.C. Lee, Gravity controlled condensation on a horizontal low-fin tube, in: Institution of Chem. Eng. Symp. Ser. 1983, pp. 415–428.
[49] R.L. Webb, T.M. Rudy, M.A. Kedzierski, Prediction of the condensation coefficient on horizontal integral-fin tubes, ASME J. Heat Transfer 107 (2) (1985) 369–376.
[50] A. Briggs, J.W. Rose, Effect of fin efficiency on a model for condensation heat transfer on a horizontal, integral-fin tube, Int. J. Heat Mass Transfer 37 (Supplement 1) (1994) 457–463.
[51] J. Mitrovic, Condensation of pure refrigerants R12, R134a and their mixtures on a horizontal tube with capillary structure: An experimental study, Forschung im Ingenieurwesen 64 (12) (1999) 345–359.
[52] M. Belghazi, A. Bontemps, C. Marvillet, Condensation heat transfer on enhanced surface tubes: experimental results and predictive theory, ASME J Heat Transfer 124 (4) (2002) 754–761.
[53] M. Belghazi, A. Bontemps, C. Marvillet, Filmwise condensation of a pure fluid and a binary mixture in a bundle of enhanced surface tubes, Int. J. Therm. Sci. 41 (7) (2002) 631–638.
[54] D.C. Zhang, W.T. Ji, W.Q. Tao, Condensation heat transfer of HFC134a on horizontal low thermal conductivity tubes, Int. Commun. Heat Mass Transfer 34 (8) (2007) 917–923.
[55] http://www.wlv.com/wp-content/uploads/2014/03/TurboBIII.pdf.